Journal of the Taiwan Institute of Chemical Engineers 000 (2017) 1–5

Contents lists available at ScienceDirect

Journal of the Taiwan Institute of Chemical Engineers

journal homepage: www.elsevier.com/locate/jtice

Nanoplasmonic Au/Ag/Au nanorod arrays as SERS-active substrate for the detection of pesticides residue

Kundan Sivashanmugan[a], Han Lee[a], Chiu-Hua Syu[a], Bernard Hao-Chih Liu[a,b], Jiunn-Der Liao[a,b,*]

[a] Department of Materials Science and Engineering, National Cheng Kung University, 1 University Road, Tainan 70101, Taiwan
[b] Center for Micro/Nano Science and Technology, National Cheng Kung University, 1 University Road, Tainan 70101, Taiwan

ARTICLE INFO

Article history:
Received 11 October 2016
Revised 15 February 2017
Accepted 20 March 2017
Available online xxx

Keywords:
Pesticides
Surface-enhanced Raman spectroscopy
Focus-ion beam
Nanorods
Nanocavity

ABSTRACT

Trace analysis of pesticides' residue found in an agricultural product is a vital topic, which is still a time-consuming and unreliable approach. A fast and effective chemical sensing technique is therefore required. Surface-enhanced Raman spectroscopy (SERS) has been well developed for detecting target species at *e.g.*, single molecule level. Herein, we used focus-ion beam and nano-indentation methods for fabricating Au/Ag/Au nanorods (NRs) and Au nanocavity array for subsequent SERS applications. The as-prepared SERS-active substrate was firstly evaluated by different wavelengths of Raman laser using rhodamine 6G as a probe molecule at low concentrations. The optimized Au/Ag/Au NRs array exhibited a strong SERS effect with an enhancement factor of 2.15×10^8. Furthermore, Au/Ag/Au NR substrates were competent to detect various types of pesticides' residue, *i.e.*, permethrin, cypermethrin, carbaryl, and phosmet at low concentrations. Presumably high SERS signals may occur at the interface between pesticide molecules and NRs surface.

1. Introduction

Permethrin, cypermethrin, carbaryl, and phosmet are commonly applied for fruits and vegetables farming and also for postharvest treatments [1,2]. Pesticide contamination in food and in the environment attracted great public concern, since it causes toxicity to human [1,3]. Many traditional methods are available to verify pesticide residues in food and vegetables. Those include mass spectrometry, capillary electrophoresis and chromatography [4–6]. However, these methods usually require complicated procedures for sample preparation. They are also time consuming, and expensive for repetitive tests.

Recently, surface-enhanced Raman scattering (SERS) gained importance for trace analysis of target species from various samples. Applications include biology, chemistry, medicine, etc., and provide high sensitivity and selectivity [7–11]. According to theoretical calculations and the literature, the electromagnetic (EM) effect is mainly contributed to the SERS enhancement. The best results revealed themselves between adjacent metal nanoparticles/nanostructures (NPs/NSs) (such as Au, Ag and Cu) [12]. Many methods including physical, (*i.e.*, e-beam lithography and focused ion beam) and chemical (*i.e.*, colloidal and electrochemical) have been utilized to fabricate high order NSs for improved sensitivity, stability, and reproducibility [12,13]. The obtainable SERS substrates are too complicated to generate a strong SERS signal. The SERS method has been used to examine pesticide residues in fruits and vegetables via Au, Ag NPs or NSs based on SERS substrates [14,15]. However, still repetitive same SERS signal from SERS substrate is key challenge in real time application.

In our group, we have developed noble metal and bimetallic NSs based SERS substrates for multidisciplinary applications. In this work, we use nano-indentation and focus ion beam (FIB) methods to fabricate Au nanocavitys (NCs) and Au/Ag/Au nanorods (NRs) arrays for creating SERS-active substrates. Notably, the physical methods are highly preventing samples from chemical or residual contaminations and provide a large density of Raman hot-spot areas. Our optimized NRs substrate was applied for pesticides detection.

2. Experimental section

2.1. Fabrication of Au nanocavity and Au/Ag/Au nanorod arrays

Au (≈100-nm-thick) and Au/Ag/Au multilayered thin films (≈30/50/320-nm-thick) were prepared by an electron beam evaporator onto a polished single-crystal silicon (1 0 0) wafer primed with a 15-nm-thick titanium adhesion layer. The Au and Au/Ag/Au

* Corresponding author.
E-mail address: jdliao@mail.ncku.edu.tw (J.-D. Liao).

http://dx.doi.org/10.1016/j.jtice.2017.03.022
1876-1070/

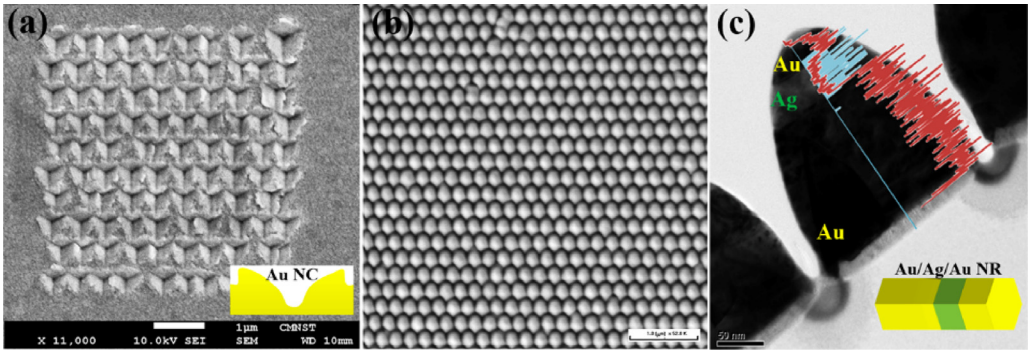

Fig. 1. FE-SEM images of as-fabricated Au NCs (a) and Au/Ag/Au NRs arrays (b). HRTEM image of Au/Ag/Au NRs with EDS mapping along the NR surface.

thin films exhibited (1 1 1) crystal orientation and an average roughness of Ra ≈ 0.82 nm. In the first step, the nano-indented cavities on thin Au films were fabricated using a dynamic contact module (DCM) system (Nanoindenter G200, Agilent Technologies, USA) in one-step loading-unloading mode. The loading and experimental parameters were described in detail in our previous publication and **Supplementary Data (SD)** [16]. The one-step loading on Au surface produced inverse pyramid shape Au NCs due to *Berkovich* tip (radius ≈20 nm). The Au NCs geometry was optimized via vertical displacement (Dv) and tip-to-tip displacement (Dt–t) for indentation. The Au/Ag/Au NRs pattern was implemented by applying an FIB (SMI 3050, SII Nanotechnology, and Japan). The pattern size was about 14 μm × 14 μm. The beam conditions included 30 kV acceleration voltage with UFine, 0.07 μm depth, 10 Pa aperture, 70 μs dwell time, +0.56 OL fine, and 8-image scale with 50% overlap [17]. The NRs geometry and experimental parameters were carried over from our previous publication [17,18]. The morphology of NCs and NRs were determined by a field-emission scanning electron microscope (FE-SEM, JSM-7001, JEOL, and Japan) and by high-resolution field-emission transmission electron microscopy (HR-FETEM, JEM-2100F JEOL, Japan).

2.2. Molecular probe and MG detection

Rhodamine 6G (R6G), the molecular probe, was diluted in aqueous solution to a concentration of 10^{-5} M. To verify the SERS effect of the Au NCs and Au/Ag NRs array substrates, the solution containing molecular probe was covered with a glass slide and then immediately measured the Raman spectra. The Raman spectra were then acquired using a confocal microscopy Raman spectrometer (Renishaw, United Kingdom) using argon ion, He-Ne and diode lasers with excitation wavelengths of 514, 633 and 785 nm, respectively. An air-cooled CCD was used as the detector; the incident power was 3 mW. The samples with the target probe-containing solution was then scanned with an integration time of 10 s over an area of 1 μm × 1 μm (the size of the laser spot was ~1 μm), using a 50× objective. The optimized Au/Ag/Au NRs substrates were further examined using four types of pesticides, namely permethrin, cypermethrin, carbaryl, and phosmet. An aqueous solution of each pesticide was diluted to a concentration of 10^{-5} to 10^{-8} M. 10 μL from each dilution of pesticides was placed on the corresponding samples.

The SERS enhancement factor (EF) was estimated according to the standard equation: [12]

$$EF = \frac{I_{sers}}{I_{bulk}} \times \frac{N_{bulk}}{N_{sers}}, \quad (1)$$

where I_{sers} and I_{bulk} are the SERS and the normal Raman scattering intensities, respectively, while N_{sers} and N_{bulk} are the number of molecules contributing to the inelastic scattering intensity, evaluated by SERS and normal Raman scattering measurements, respectively. The SERS spectra were averaged from 10 consecutive measurements on different samples. All Raman spectra's were normalized by using peak fit software.

3. Results and discussion

3.1. Characterization of Au NCs and Au/Ag/Au NRs array

The morphology of Au NCs and Au/Ag/Au NRs arrays were respectively characterized by FE-SEM. In Fig. 1(a), FESEM images, the depth D_v (≈ 90 nm) and the distance D_{t-t} (≈500 nm) of Au NCs array substrates were distinguishable. The individual cavities with three pile-up regions were produced during the one-step indentation loading method, as shown in Fig. 1(a). The reverse pyramid-shape NCs were mostly generated the surface plasmons resonance (SPR) due to the high electrons generated around the NCs [16]. Fig. 1(b) shows FESEM images of top-views about Au/Ag/Au NRs substrate. The geometry of NRs (*i.e.*, shape, length and spacing) was controlled by adjusting etching time and the operating current during FIB fabrication. The optimization regarding the NRs geometry was obtained in our previous publication [17,18]. The NR shape, length, diameter, and spacing between two NRs were hexagonal, 400 nm (top layer Au, 30 nm, embedded Ag layer 50 nm, bottom Au layer 320 nm), 170 nm and 30 nm with a pattern size of 14 μm × 14 μm, as shown in Fig. 1(b) and (c). The NRs were composed in a single layer (Au/Ag/Au) without alloying. This is also apparent from the Energy-dispersive X-ray spectroscopy (EDS) line mapping along the NRs surface, as shown in Fig. 1(c).

In Fig. S2(a) and (b) in SD, the Au NCs and Au/Ag/Au NRs samples with a concentration of 10^{-5} M R6G solution were examined by Raman spectroscopy with different laser wavelengths. The most characteristic peak at 1362 cm^{-1} (ν(C=C), aromatics) was used to compare the effects of the Raman laser and the SERS-active substrates, as shown in Fig. S2(c) in SD. The triangular Au NCs arrays substrate SPR was highly matched with 633 nm Raman laser and enhanced SERS effect, as compared to the 514 and 785 nm Raman lasers. We found the Au NCs sample EF close to 1.63×10^7. Notably, the NCs parameters Dv and D_{t-t} can influence the SERS effect. In the case of Au/Ag/Ag NR samples, the strongest SERS effect was obtained by 785 nm Raman laser due to a strong lightning rod effect with matched SPR field enhancement, where EF reached nearly 2.15×10^8.

In addition, the NCs and NRs array samples were utilized to determine the low concentration of R6G as 10^{-8} M. The NRs substrate exhibited a strong Raman intensity compared with NCs, as shown in Fig. 2 and Fig. S3 in SD. However, the multilayer NRs revealed long range optical properties (*i.e.*, visible in the near-infrared regions). This is due to the embedded Ag layer influencing the local field EM around the two consecutive NRs interface, which

Please cite this article as: K. Sivashanmugan et al., Nanoplasmonic Au/Ag/Au nanorod arrays as SERS-active substrate for the detection of pesticides residue, Journal of the Taiwan Institute of Chemical Engineers (2017), http://dx.doi.org/10.1016/j.jtice.2017.03.022